Brain Imaging and Behavior
https://doi.org/10.1007/s11682-018-9838-8

ORIGINAL RESEARCH

Common and distinct changes of default mode and salience network in schizophrenia and major depression

Junming Shao[1,2,3,4] · Chun Meng[5,6] · Masoud Tahmasian[7] · Felix Brandl[5,6] · Qinli Yang[3] · Guangchun Luo[2] · Cheng Luo[1] · Dezhong Yao[1] · Lianli Gao[2] · Valentin Riedl[4,5,6] · Afra Wohlschläger[5,6] · Christian Sorg[5,6,8]

Abstract

Brain imaging reveals schizophrenia as a disorder of macroscopic brain networks. In particular, default mode and salience network (DMN, SN) show highly consistent alterations in both interacting brain activity and underlying brain structure. However, the same networks are also altered in major depression. This overlap in network alterations induces the question whether DMN and SN changes are different across both disorders, potentially indicating distinct underlying pathophysiological mechanisms. To address this question, we acquired T1-weighted, diffusion-weighted, and resting-state functional MRI in patients with schizophrenia, patients with major depression, and healthy controls. We measured regional gray matter volume, inter-regional structural and intrinsic functional connectivity of DMN and SN, and compared these measures across groups by generalized Wilcoxon rank tests, while controlling for symptoms and medication. When comparing patients with controls, we found in each patient group SN volume loss, impaired DMN structural connectivity, and aberrant DMN and SN functional connectivity. When comparing patient groups, SN gray matter volume loss and DMN structural connectivity reduction did not differ between groups, but in schizophrenic patients, functional hyperconnectivity between DMN and SN was less in comparison to depressed patients. Results provide evidence for distinct functional hyperconnectivity between DMN and SN in schizophrenia and major depression, while structural changes in DMN and SN were similar. Distinct hyperconnectivity suggests different pathophysiological mechanism underlying aberrant DMN-SN interactions in schizophrenia and depression.

Keywords Functional MRI · Diffusion tensor imaging · Schizophrenia · Depression · Default mode network · Salience network

Introduction

Brain imaging has revealed that schizophrenia is a disorder of macroscopic brain networks (Palaniyappan and Liddle 2012; Schmidt et al. 2014; Stephan et al. 2009; van den Heuvel and Fornito 2014; Chen et al. 2015; Williamson 2007). Prominent functional and structural changes have been found particularly in the default mode and salience network (DMN, SN) (Manoliu et al. 2013a, b, 2014; Orliac et al. 2013; Wang et al. 2015; Whitfield-Gabrieli et al. 2009;

✉ Christian Sorg
christian.sorg@tum.de

[1] Center for Information in BioMedicine, University of Electronic Science and Technology of China, 611731 Chengdu, China

[2] School of Computer Science and Engineering, University of Electronic Science and Technology of China, 611731 Chengdu, China

[3] Big Data Research Center, University of Electronic Science and Technology of China, 611731 Chengdu, China

[4] Department of Nuclear Medicine, University of Electronic Science and Technology of China, 611731 Chengdu, China

[5] Department of Neuroradiology, Technische Universität München, Ismaninger Strasse 22, 81675 Munich, Germany

[6] TUM-Neuroimaging Center of Klinikum rechts der Isar, Technische Universität München, Ismaninger Strasse 22, 81675 Munich, Germany

[7] Institute of Medical Science and Technology, Shahid Beheshti University, Tehran, Iran

[8] Department of Psychiatry, Klinikum rechts der Isar Technische Universität München, Ismaninger Strasse 22, 81675 Munich, Germany

Published online: 19 February 2018

Wotruba et al. 2014). Both networks are intrinsic brain networks characterized by the coherence of slowly fluctuating ongoing activity (< 0.1 Hz), which is called intrinsic functional connectivity (iFC) and typically measured by correlated blood oxygenation fluctuations during resting-state functional MRI (rs-fMRI) (Biswal et al. 1995; Fox and Raichle 2007). DMN and SN, however, are impaired not only in schizophrenia but also in major depression (Bora et al. 2012; Frodl et al. 2008; Kaiser et al. 2015; Kieseppä et al. 2010; Liao et al. 2013; Manoliu et al. 2013a, b). This overlap of network changes induces the question whether changes of DMN and SN are common or different across schizophrenia and depression. More specifically, the current study addresses the question of which changes in functional connectivity and underlying gray and white matter of cortical DMN and SN differ across both disorders, potentially indicating distinct underlying pathophysiological mechanisms. To justify and address this specific question, we first review most consistent functional and structural changes of intrinsic brain networks in schizophrenia and major depression, and then describe our study procedure.

Changes of iFC in the DMN, covering medial prefrontal and parietal areas, the SN, covering cingulo-operculo-insular cortices, and the so-called central executive network (CEN), covering lateral frontal and parietal cortices, have been consistently observed in schizophrenia (Dong et al. 2017; Manoliu et al. 2013a, b, 2014; Orliac et al. 2013; Wang et al. 2015; Whitfield-Gabrieli et al. 2009; Wotruba et al. 2014). IFC within and between DMN, SN, and CEN is impaired in persons at high-risk for schizophrenia (Wotruba et al. 2014), psychotic patients (Manoliu et al. 2014), and remitted patients with chronic schizophrenia (Manoliu et al. 2013a, b). Grey matter volume loss in schizophrenia is focused on insula and anterior cingulate cortices (ACC), which are both part of the SN and partly of the DMN (Borgwardt et al. 2007; Ellison-Wright et al. 2008). White matter tract changes (i.e., mainly decreased connectivity) affect particularly frontal and temporal lobes, which include fiber tracts connecting frontal lobe, insula, cingulate gyrus, and temporal cortices, thereby interconnecting DMN, SN, and CEN (Buchsbaum et al. 2006; Ellison-Wright and Bullmore 2009). DMN, SN, and CEN are also altered in major depression (Kaiser et al. 2015; Manoliu et al. 2013a, b; Mulders et al. 2015; Greicius et al. 2007; Sheline et al. 2010). Recent meta-analyses found aberrant iFC within and between DMN and SN in depression, such as anterior DMN-SN hyperconnectivity and reduced SN connectivity (Frodl et al. 2008; Mulders et al. 2015). Grey matter volume loss in the ACC is the most consistent finding in volumetric MRI studies in depression (Bora et al. 2012; Frodl et al. 2008; Goodkind et al. 2015). Correspondingly, a meta-analysis of white matter integrity identified changes around ACC and insula as most consistent changes in depression, suggesting substantial fiber changes in both DMN and SN in major depression (Kieseppä et al. 2010; Liao et al. 2013). In summary, these findings indicate changes in iFC, grey and white matter of DMN, SN, and CEN in both schizophrenia and depression, with highest consistency of changes in cortical parts of DMN and SN.

To address the question of distinct DMN and SN alterations in schizophrenia and depression, we focused on cortical DMN and SN regions in patients of each disorder as well as in healthy controls. We measured networks' regional gray matter volume (GMV) by the use of T1-weighted MRI and voxel-based morphometry (VBM), structural connectivity (SC) by diffusion-weighted MRI and inter-regional fiber-tracking, and iFC by resting-state functional MRI and inter-regional correlations of fMRI signals, respectively. In order to identify group differences in network properties across modalities, we applied an identical group comparison methodology for each modality (for overview see Fig. 1): firstly, we used the same region-of-interest (ROI)-based network approach for each modality; specifically, DMN and SN were defined by a-priori cortical ROIs (Fig. 2; Table 2) and for each ROI or ROI-ROI-pair, GMV, SC, and iFC were determined. Please note that our single-ROI-approach on grey matter volume is based on foregoing whole-brain VBM, which is then restricted to selected ROIs. Secondly, since this procedure resulted in multi-variate outcome measures for each modality (e.g. a ROI vector for GMV and a ROI–ROI connectivity matrix for iFC and SC), we applied generalized Wilcoxon rank testing for each modality, respectively (Hahn et al. 2013). Wilcoxon rank testing allows for reducing multi-variate data to uni-variate data while preserving accurate statistical testing. Thirdly, to exclude effects of current symptoms on network differences across patient groups, we controlled for these effects via linear regression; this procedure allowed us to focus on network changes due to potentially distinct underlying pathophysiology, instead of distinct symptom states in schizophrenia and depression. Fourthly, to exclude effects of age, sex, and medication, we controlled these effects via linear regression.

Materials and methods

Subjects

21 patients with schizophrenia, 25 patients with major depression, and 25 healthy controls participated in the study (Table 1). The study was approved by the local Ethics Committee of Technische Universität München, Klinikum rechts der Isar. All participants provided informed consent in accordance with the Human Research Committee guidelines of Technische Universität München. Patients were in-patients and recruited from the Department of Psychiatry by treating psychiatrists, healthy controls from the area of

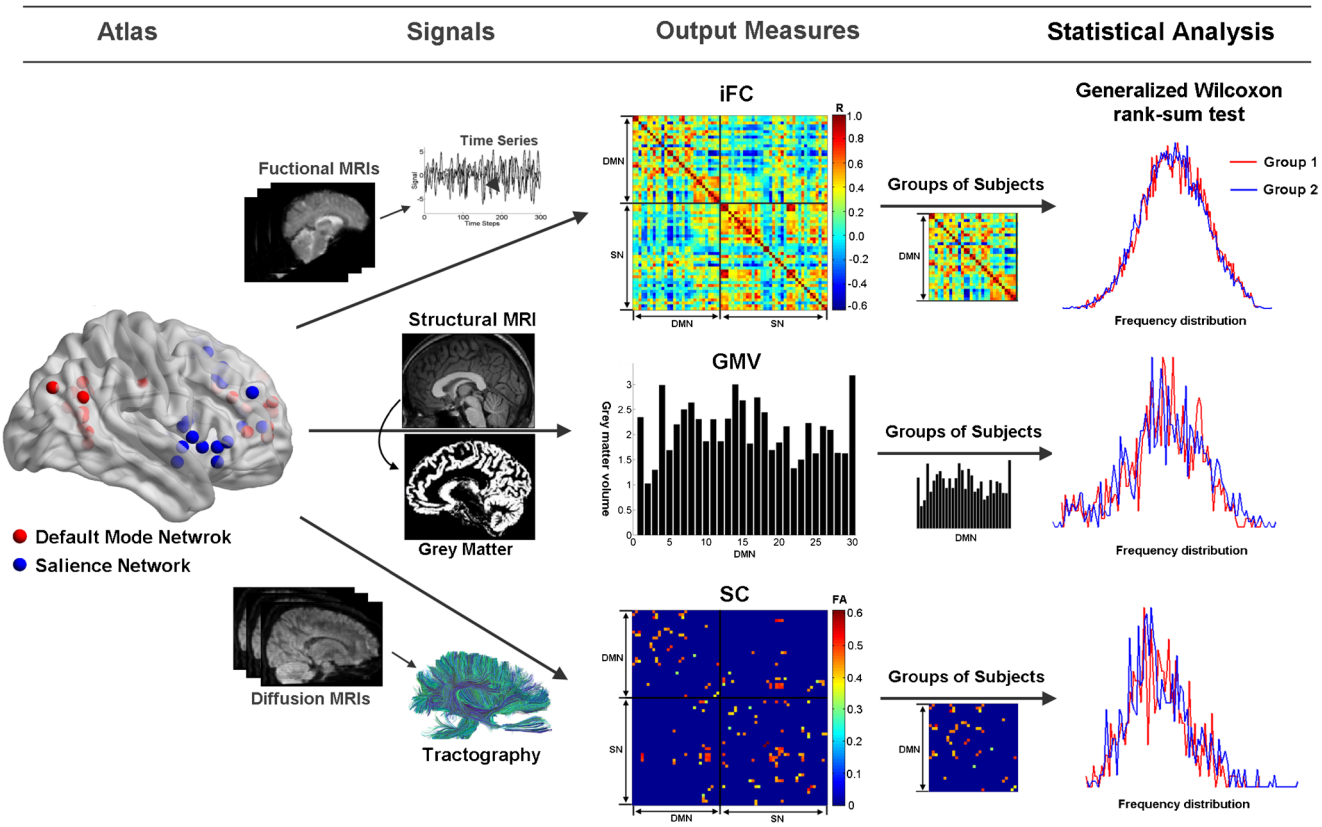

Fig. 1 Flow-chart of multi-modal imaging approach on default mode and salience network (DMN, SN) in schizophrenia and depression. iFC intrinsic functional connectivity, GM grey matter, SC structural connectivity

Munich by word-of-mouth advertising. Participants' examination included medical history, psychiatric interview, and psychometric assessment. Psychiatric diagnoses were based on DSM-IV (American Psychiatric Association 2000). The Structured Clinical Interview for DSM-IV was used to assess the presence of psychiatric diagnoses (Spitzer et al. 1992). Severity of clinical symptoms was measured with the Hamilton Rating Scale for Depression (Hamilton 1960) and the Positive and Negative Symptom Scale (Kay et al. 1987). The global level of social, occupational, and psychological functioning was measured with the Global Assessment of Functioning Scale (Spitzer et al. 1992). Psychiatrists D.S. and M.S. performed clinical-psychometric assessment; they have been professionally trained for Structured Clinical Interviews for DSM-IV with inter-rater reliability for diagnoses and scores of more than 95%.

For schizophrenic patients, schizophrenia was the primary diagnosis. All patients included were diagnosed with paranoid schizophrenia during acute psychosis as indicated by clinical exacerbation and increased positive symptom scores on the PANSS. Due to increased vulnerability of psychotic patients, treating psychiatrists ensured very carefully that patients were able to provide informed consent for the study. Patients were free of any current or past depressive or manic episode, major depression, bipolar disorder, and substance abuse. For depressive patients, major depression was the primary diagnosis. These patients had recurrent major depression with current depressive episode. They were free of current or past psychotic symptoms, schizophrenia, schizoaffective disorder, bipolar disorder, and substance abuse. All healthy controls were free of any current or past neurological or psychiatric disorder or psychotropic medication. More detailed information about patients please refer to Table 1.

MRI data acquisition

All subjects underwent T1-weighted, diffusion-weighted (DTI, diffusion tensor imaging), and resting-state-functional MRI (rs-fMRI) in a 3T Philips Achieva using an eight-channel phased-array head coil. T1-weighted structural data were obtained using a magnetization-prepared rapid acquisition gradient echo sequence (TE = 4 ms, TR = 9 ms, TI = 100 ms, flip angle = 5°, FoV = 240 × 240 mm², matrix = 240 × 240, 170 slices, voxel size = 1 × 1 × 1 mm). Diffusion weighted MRI was based on a pulsed gradient spin-echo echo planar imaging sequence with a parallel imaging (SENSE) factor of 2.5, TE = 60 ms, TR = 6516 ms, 60 contiguous slices

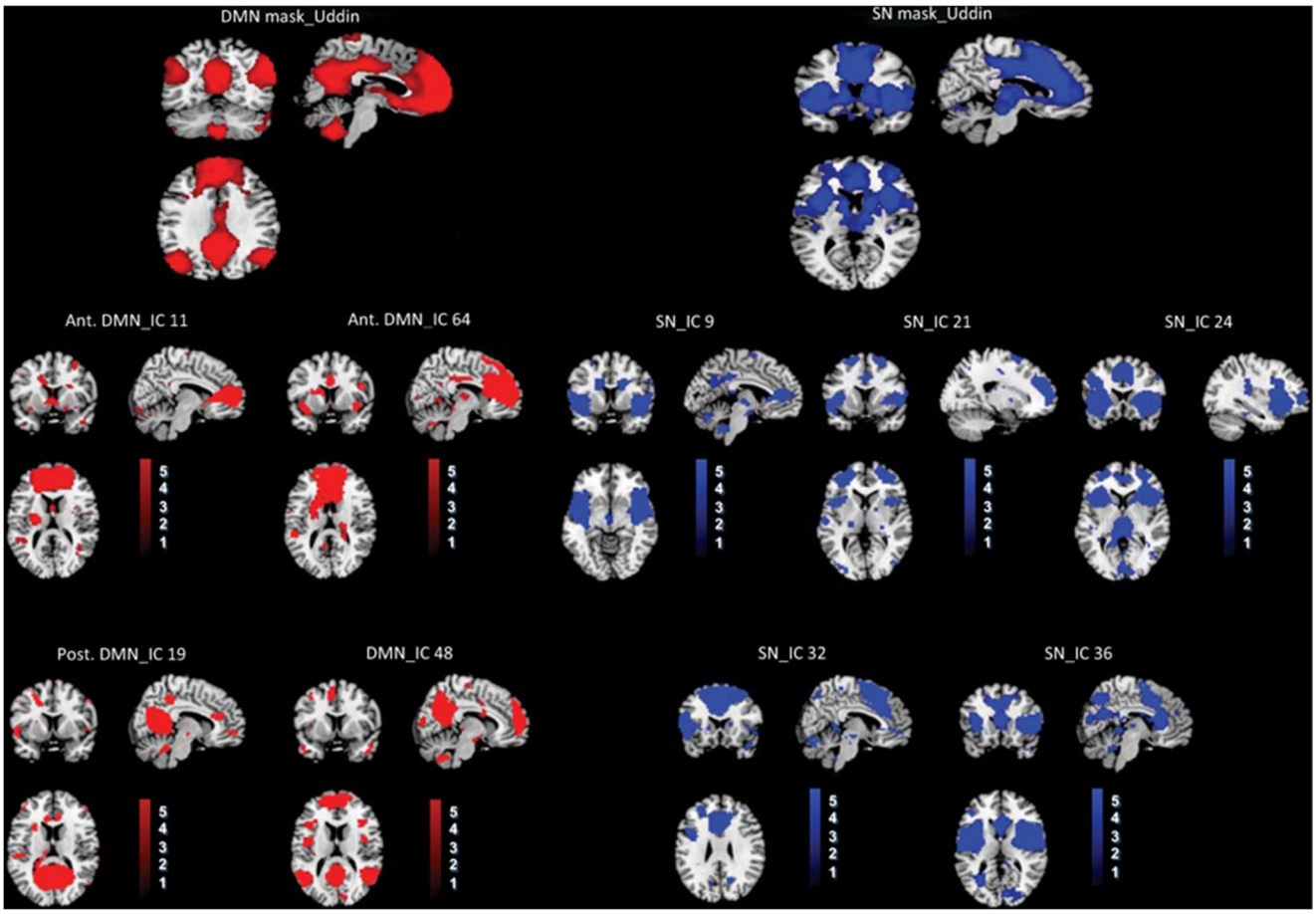

Fig. 2 DMN and SN templates and selected networks of interest. Above row: T-maps of DMN and SN based on Uddin templates (Uddin et al. 2011). Middle and below row: T-maps of selected components representing DMN and SN (one-sample t-test, $p < 0.05$ FWE corrected). Components are based on high-model order ICA of fMRI data from healthy controls. Selection is based on spatial regression of components on Uddin templates

Table 1 Demographic and clinical characteristics

	SZP (n = 21)	MDD (n = 25)	Controls (n = 25)	p1
Age (years)	35.3 (12.5)	48.8 (14.8)	41.8 (17.6)	< 0.05
Sex (f/m)	9/9	13/12	15/10	
PANSS, total	76.4 (18.5)	35.2 (3.4)	30.2 (0.8)	< 0.01
PANSS, positive	18.1 (5.7)	7.8 (1.1)	7.05 (0.24)	< 0.01
PANSS, negative	19.9 (8.1)	10.0 (2.3)	7.11 (0.48)	< 0.01
HAM-D	9.0 (5.9)	22 (7.1)	0.5 (0.9)	< 0.01
GAF	41.5 (11.6)	50 (10.5)	99.5 (1.1)	< 0.01

[1]Statistical testing was based on ANOVA. Abbreviations: SZP schizophrenia; MDD major depressive disorder; PANSS, Positive and Negative Syndrome Scale; Ham-D Hamilton depression scale; GAF Global Assessment of Functioning Scale

with112 × 112 matrix size of slice (subsequently reconstructed for a128 × 128 matrix size, with a resolution of 1.75 mm in plane and a slice thickness of 2 mm resulting in 128 × 128 × 60 voxels with size 1.75 × 1.75 × 2 mm^3), diffusion gradients in 15 non–collinear directions with b = 800 s/mm^2; B0 image without diffusion weighting, b = 0 s/mm^2, was additionally acquired. Rs-fMRI data were collected using a gradient EPI sequence (TE = 35 ms, TR = 2000 ms, flip angle = 82°, FoV = 220 × 220 mm^2, matrix = 80 × 80, 32 slices, slice thickness = 4 mm, and 0 mm interslice gap; 10 min of scanning result in 300 volumes).

Definition of network nodes

To define nodes of DMN and SN, an independent sample of 25 healthy controls (mean age 25. 5 years, 12 females) without any psychiatric, neurological and systemic disease was assessed by T1-weighted and resting-state functional MRI at the same scanner and with the same sequences

Table 2 Nodes of default mode and salience network

ID	Name	Abbreviation	Size	T-value	P-value	x	y	z
A: Default Mode Network								
1	L Middle Occipital Gyrus	L MOG	46	21.30	<0.001	-39	-75	33
2	L Cuneus	L Cuneus	86	20.35	<0.001	-9	-66	21
3	L Lingual Gyrus	L Lingual	80	18.30	<0.001	-9	-54	-1
4	L Inferior Precuneus	L Inf Precuneus	239	24.58	<0.001	-9	-57	9
5	L Middle Precuneus	L Mid Precuneus	153	30.42	<0.001	-9	-60	18
6	LSuperior Precuneus	L Sup Precuneus	337	23.69	<0.001	-3	-63	30
7	L Angular Gyrus	L Angular	83	14.08	<0.001	-48	-60	30
8	L Posterior Cingulate Cortex	L PCC	78	25.18	<0.001	-3	-54	30
9	L Posterior Midcingulate Cortex	L Post MCC	45	12.78	<0.001	0	-21	36
10	L Dorsal Anterior Cingulate	L dACC	286	24.33	<0.001	-6	33	27
11	L Genual Anterior Cingulate	L gACC	135	22.81	<0.001	-15	39	6
12	L Inferior Dorsolateral PFC	L Inf dlPFC	59	12.31	<0.001	-24	54	3
13	L Superior Dorsolateral PFC	L Sup dlPFC	86	11.35	<0.001	-12	51	39
14	L Inferior Dorsomedial PFC	L Inf dmPFC	96	17.49	<0.001	-6	51	9
15	L Middle Dorsomedial PFC	L Mid dmPFC	77	11.43	<0.001	0	57	18
16	L Superior Dorsomedial PFC	L Sup dmPFC	403	25.82	<0.001	0	42	21
17	R Superior Dorsomedial PFC	R Sup dmPFC	81	13.06	<0.001	6	57	24
18	R Middle Dorsomedial PFC	R Mid dmPFC	307	17.14	<0.001	3	54	21
19	R Inferior Dorsomedial PFC	R Inf dmPFC	101	13.67	<0.001	18	54	3
20	R Superior Dorsolateral PFC	R Sup dlPFC	110	14.15	<0.001	18	45	30
21	R Inferior Dorsolateral PFC	R Inf dlPFC	83	13.09	<0.001	24	54	9
22	R Genual Anterior Cingulate	R gACC	141	19.23	<0.001	12	42	6
23	R Dorsal Anterior Cingulate	R dACC	313	20.95	<0.001	6	33	27
24	R Anterior Midcingulate Cortex	R Ant MCC	71	13.18	<0.001	3	24	33
25	R Angular Gyrus	R Angular	111	16.23	<0.001	51	-57	27
26	R Superior Precuneus	R Sup Precuneus	288	23.88	<0.001	6	-57	36
27	R Inferior Precuneus	R Inf Precuneus	229	26.95	<0.001	6	-57	18
28	R Lingual Gyrus	R Lingual	124	26.83	<0.001	9	-54	6
29	R Calcarine Sulcus	R Calcarine	222	26.46	<0.001	15	-57	15
30	R Middle Occipital Gyrus	R MOG	38	16.41	<0.001	42	-75	33
B: Salience Network								
1	L Superior Temporal Gyrus 2	L STG 2	63	14.60	<0.001	-51	-6	3
2	L Superior Temporal Gyrus 1	L STG 1	172	25.79	<0.001	-48	6	-3
3	L Superior Temporal Pole	L STP	76	16.56	<0.001	-45	9	-15
4	L Posterior Insula	L Post Insula	188	23.03	<0.001	-39	3	9
5	L Middle Insula	L Mid Insula	168	19.40	<0.001	-45	12	-6
6	L Anterior Insula	L Ant Insula	199	26.88	<0.001	-30	24	0
7	L Rolandic Operculum	L Rol Operculum	162	21.11	<0.001	-54	3	12
8	L Frontal Operculum	L Fr Operculum	144	15.70	<0.001	-45	9	15
9	L Midcingulate Cortex	L MCC	68	21.7	<0.001	-6	24	36
10	L Anterior Cingulate Cortex	L ACC	35	16.02	<0.001	0	39	9
11	L Lateral Orbitofrontal Cortex	L Lat OFC	127	17.33	<0.001	-30	24	-12
12	L Ventrolateral PFC	L vlPFC	59	21.02	<0.001	-33	30	0
13	L Posterior Inferior Dorsolateral PFC	L Post Inf dlPFC	536	19.10	<0.001	-36	39	18
14	L Anterior Inferior Dorsolateral PFC	L Ant Inf dlPFC	101	13.01	<0.001	-27	54	0
15	L Posterior Superior Dorsolateral PFC 2	L Post Sup dlPFC 2	96	12.51	<0.001	-33	6	57
16	L Posterior Superior Dorsolateral PFC 1	L Post Sup dlPFC 1	165	14.41	<0.001	-18	9	54
17	L Anterior Superior Dorsolateral PFC 3	L Ant Sup dlPFC 3	153	14.63	<0.001	-18	12	60
18	L Anterior Superior Dorsolateral PFC 2	L Ant Sup dlPFC 2	310	20.91	<0.001	-9	18	57
19	L Anterior Superior Dorsolateral PFC 1	L Ant Sup dlPFC 1	110	16.22	<0.001	-12	24	57

Table 2 (continued)

ID	Name	Abbreviation	Size	T-value	P-value	x	y	z
20	L Dorsomedial PFC	L dmPFC	135	17.32	<0.001	-3	27	36
21	R dmPFC 1	R dmPFC 1	58	15.53	<0.001	6	27	45
22	R Dorsomedial PFC 2	R dmPFC 2	73	17.62	<0.001	6	24	42
23	R Superior Dorsolateral PFC	R Sup dlPFC	269	26.95	<0.001	6	18	54
24	R Middle Dorsolateral PFC	R Mid dlPFC	444	21.25	<0.001	30	45	30
25	R Inferior Dorsolateral PFC	R Inf dlPFC	105	12.30	<0.001	30	51	9
26	R Ventrolateral PFC	R vlPFC	62	27.23	<0.001	39	30	0
27	R Lateral Orbitofrontal Cortex	R Lat OFC	124	18.44	<0.001	36	24	-12
28	R Anterior Cingulate Cortex	R ACC	34	16.86	<0.001	3	39	9
29	R Midcingulate Cortex 1	R MCC 1	83	18.34	<0.001	6	24	39
30	R Midcingulate Cortex 2	R MCC 2	78	12.20	<0.001	9	27	36
31	R Frontal Operculum	R Fr Operculum	154	18.27	<0.001	57	9	3
32	R Rolandic Operculum	R Rol Operculum	202	21.11	<0.001	45	3	9
33	R Anterior Insula	R Ant Insula	164	27.23	<0.001	36	24	-3
34	R Middle Insula	R Mid Insula	206	18.44	<0.001	39	15	-3
35	R Posterior Insula	R Post Insula	197	19.89	<0.001	36	6	12
36	R Superior Temporal Pole	R STP	76	15.21	<0.001	54	3	-3
37	R Superior Temporal Gyrus	R STG	70	16.57	<0.001	48	0	-12

as the study sample. The first three functional images of each subject were discarded due to magnetization effects. Remaining fMRI data were preprocessed by SPM8 (Wellcome Department of Cognitive Neurology, London) including head motion correction, spatial normalization into the standard stereotactic space of the Montreal Neurological Institute with isotropic voxel of $3\times3\times3$ mm^3, and spatial smoothing with a $6\times6\times6$ mm^3 Gaussian kernel to reduce spatial noise. To ensure data quality, particularly concerning motion-induced artifacts, point-to-point head motion were estimated for each subject. Excessive head motion (cumulative motion translation or rotation > 3 mm or 3° and mean point-to-point translation or rotation > 0.15 mm or 0.1°) was applied as exclusion criterion. Point-to-point motion was defined as the absolute displacement of each brain volume compared to its previous volume. None of the participants had to be excluded.

Following the approach of Allen et al. (Allen et al. 2011), preprocessed data were decomposed into 75 spatial independent components within a group-ICA framework, based on the infomax-algorithm and implemented in the GIFT-software (http://icatb.sourceforge.net). High-model-order ICA approaches yield independent components, which are in accordance with known anatomical and functional segmentation (Abou-Elseoud 2010). FMRI data were concatenated and reduced by two-step principal component analysis, followed by independent component estimation with the infomax-algorithm. We subsequently ran 20 ICA (ICASSO) to ensure stability of the estimated components. This results in a set of average group components, which are then back reconstructed into single subject space. Each back-reconstructed component consists of a spatial z-map reflecting component's functional connectivity pattern across space and an associated time course reflecting component's activity across time.

To select the independent components reflecting networks of interest in an automated and objective way, we conducted multiple spatial regressions on 75 independent components' spatial maps using T-maps of DMN and SN from Uddin (Uddin et al. 2011) (Fig. 2 first row) For each network, independent components with highest correlation coefficients and positive visual inspection by two independent raters (C.S., V.R.) were chosen, resulting in 9 components of interest: 4 components reflecting DMN, and 5 reflecting subsystems of the SN (Fig. 2 middle and last row).

In order to define representative nodes (i.e. regions-of-interest ROIs) for DMN and SN, each component representing DMN and SN was split into several ROIs. Specifically, for each selected component, major clusters in the components were first identified by using *xjview* toolbox (http://www.alivelearn.net/xjview) and SPM8. If the volume of the cluster is above 30 voxels, the coordinate with peak value with significance in this region was extracted. Then, all obtained coordinates were used as centers to generate 3 mm-radius regions of interest (ROIs).Finally, all ROIs defined in this way were carefully visually inspected to exclude spatial overlap between distinct ROIs.

Definition of regional and inter-regional outcome measures

Voxel-based morphometry (VBM) and regional GMV. To evaluate GMV of network nodes, VBM of T1-weighted MRI

data was performed (Sorg et al. 2013). In brief, by the use of VBM8 toolbox (http://dbm.neuro.uni-jena.de/vbm.html), T1-weighted images were corrected for bias-field inhomogeneity, registered using linear (12-parameter affine) and nonlinear transformations, and tissue-classified into gray matter, white matter, and cerebro-spinal fluid within the same generative model. Of the resulting images, the modulated gray-matter images were selected for further analysis in order to account for volume changes resulting from the normalization process. Here, we only considered non-linear volume changes so that further analyses did not have to account for differences in head size. Images were smoothed with a Gaussian kernel of 8 mm, and network ROIs were used to define individual GMV values.

Diffusion-based tractography and SC. To evaluate tract-based SC across network nodes, tractography of individual DTI data was performed and related to cortical network ROIs (Shao et al. 2012). In brief, first, network ROIs were transformed in individual DTI space, and reduced to volumes without cerebral spinal fluid and with fractional anisotropy (FA) < 0.2 indicating gray matter. Second, after motion correction and voxel-wise diffusion tensor calculation, deterministic fiber tracking algorithm TEND (Lazar et al. 2003) was applied, with all voxels with FA > 0.3 being selected as seed points of fiber tracking (Lazar et al. 2003). Tracking stopped in voxels with FA < 0.2 or physiologically implausible curvature of the track (> 60 degrees) (Lazar et al. 2003). Third, output of both ROI-based cortical parcellation and diffusion tractography were combined to construct individual structural connectivity network for each subject. Connectivity of each pair of ROIs was measured by fibers across the two regions. If there exists at least one fiber with endpoints in one pair of regions (e.g. region *i* and region *j*), the two cortical regions are assumed to be connected (Hagmann et al.,2008). For each connection, FA_{ij} was used to reflect the weighted edge of a network, and defined as the mean value of FA across all voxels of all connection fibers between the two cortical regions.

Functional MRI signal correlation analysis and iFC. To evaluate iFC across network nodes, rs-MRI signal correlation analysis was performed following (Meng et al., 2014). After discarding the first three functional volumes for each subject, data were corrected for head motion, spatially normalized into the Montreal Neurological Institute standard stereotactic space with isotropic voxel size of $3 \times 3 \times 3$ mm^3, and spatially smoothed with a $6 \times 6 \times 6$ mm^3 Gaussian kernel to reduce spatial noise. Data quality was tested in-depth, particularly concerning motion-induced artifacts, temporal signal-to-noise ratio and point-to-point head motion, which were estimated for each subject (Van Dijk et al. 2012; Luo et al. 2015). ANOVA and post-hoc t-tests showed no significant differences between groups regarding mean point-to-point translation or rotation in any direction (ANOVA, $p > 0.19$) as well as temporal signal-to-noise ratio (ANOVA, $p > 0.40$). Then, voxel time courses and confounding time courses (i.e., six time courses of head motion and signals derived from whole grey matter, white matter and cerebro-spinal fluid) were extracted and bandpass-filtered (0.009 to 0.09 Hz). To construct iFC networks, voxel time series were averaged for each ROI and then regressed against confounding covariates. To estimate intrinsic functional connectivity among different ROIs, Pearson's correlation coefficients (R_{ij}) of corresponding time courses of any two ROIs *i* and *j*, was computed and transformed to z-values z_{ij} via r-to-z Fisher transformation. Finally, for each individual subject, iFC within and between DMN and SN, respectively, was represented by corresponding ensembles of z_{ij}.

Statistical analysis across subjects via generalized Wilcoxon test

To compare network features of GMV, SC, and iFC across groups, we applied generalized Wilcoxon rank tests (Hahn et al. 2013). In contrast to both multivariate approaches (e.g. pattern classification) and element-wise comparisons (e.g. ROI–ROI comparisons), this approach facilitates univariate across-subject comparisons of whole networks together with rigorous statistical testing (Hahn et al. 2013). To identify potential changes in a given feature (e.g. iFC) of a given network (e.g. SN), features are collected in univariate samples (e.g. iFC of all possible ROI–ROI pair combinations XY in the SN). Such samples define frequency distributions F_{XY} (SN; iFC), which are used for subsequent across subject comparisons (e.g. group–group comparison). To account for the skewness of univariate distributions F_{XY} (SN; iFC), procedures of nonparametric statistics are necessary such as generalized Wilcoxon rank-sum testing (Brunner et al. 2000). More formally, when F is defined by subjects of two groups A and B, respectively, for a given network and feature, generalized Wilcoxon rank test W_{BF} enables to decide whether the rank sum of F for the group A tends to be higher or lower from those for the group B. To obtain p-values, the test statistic W_{BF} is compared with a distribution of zero mean and unit standard deviation based on non-parametric permutation procedure (with 10,000 permutations). Results were Bonferroni corrected for multiple comparisons (i.e., 9 iFC-related comparisons + 9 SC + 6 GMV = 24 comparisons with p-threshold at 0.002).

To illustrate the group separating potential of specific brain features such as iFC of a given ROI–ROI pair, we calculated its discriminative power based on rank information. The discriminative power of one feature is defined as its mean rank difference over the number of total features between two groups. For example, given two groups A and B with the number of features *m* for each group (e.g. m iFC connections), and R_A and R_B are the mean ranks of a given

functional connection x for groups A and B, the discriminative power of this connection x is defined as $|R_A - R_B|/2\ m$.

Before across-subject comparisons, we accounted for effects of co-variates-of-no-interest on outcomes of GMV, SC, and iFC. To be independent from effects of sex, age, and medication, we regressed out these scores before group comparison. Concerning specifically medication, both antidepressant and anti-psychotic medication have been shown to influence iFC (e.g. Schaefer, Burmann et al., Current Biology 2014, Sambataro F, Blasi G et al., Neuropsychopharmacology 2010). For antipsychotics, the canonical approach to control for their effects on brain features is to make distinct antipsychotics comparable via chlorpromazine equivalent dose (CPZ) calculation and then to account for CPZ scores via linear regression (e.g. Manoliu et al. 2014). While for antipsychotics canonical CPZ mapping allows for direct comparison of distinct antipsychotics, similar approaches are not available for distinct antidepressants. Therefore with respect for antidepressant control, we followed a previously evaluated approach as described in (Meng et al., 2014) and defined categorical regressors for each antidepressant type (selective serotonin re-uptake inhibitor, serotonin-norepinephrine re-uptake inhibitor, noradrenergic and specific serotonergic antidepressants), which were then removed from outcomes. One should be aware that such linear and independent regression approach of controlling distinct medication effects is only a rough approximation of true effects, which likely include non-linear and interaction effects. Concerning comparisons across patient groups, psychiatric symptoms of patients may influence comparisons of network changes across disorders. To be independent from current symptoms when comparing patient groups, we removed effects of symptoms as reflected by psychometric scales of PANSS positive, PANSS negative, and HAM-D (see Table 1) on brain outcome measures via linear regression. This approach of controlling for symptoms follows analogous approaches of task-fMRI in different populations with distinct population performances for the task. In such studies, across-group comparisons of task-associated brain activity are typically controlled for task performance. Thereby, group differences in task-associated brain activity are independent of task performance.

Results

ICA-derived regions of interest

Based on the ICA analysis, finally 67 ROIs were generated to represent the two networks of interest: 30 ROIs for the DMN and 37 ROIs for the SN. Table 2 illustrates the used sub-regions and peak coordinates.

In comparison with healthy controls, patients show similar changes in DMN and SN for each modality

In the SN, GMV was decreased in each patient group, respectively, compared to healthy controls (Table 3, last column). In the DMN, structural connectivity was altered in patients with schizophrenia ($p = 0.005$) and depression ($p = 0.037$), respectively, in comparison with controls (Table 3, middle row). These findings did not survive correction for multiple comparisons. Within the SN, iFC was decreased in both patient groups, respectively (schizophrenia $p = 0.004$ (does not survive Bonferroni correction), depression $p < 0.001$), while iFC between SN and DMN was increased in both patient groups (Table 3, first row).

Distinct and common alterations of SN and DMN across patient groups

SN volume reductions did not differ across patient groups (Table 3, last row). Aberrant DMN structural connectivity was not different across patient groups (Table 3, middle row). SN intrinsic connectivity reductions did not differ between patients with schizophrenia and depression, respectively (Table 3, first row).iFC between SN and DMN was significantly increased in depressed patients compared to schizophrenic patients. Calculation of group discriminative power of single functional connections revealed mainly iFC between fronto-insular SN parts and posterior-parietal DMN parts among the 20 most discriminative connections (Fig. 3).

Discussion

The current study investigated whether cortical SN and DMN changes in grey matter volume, structural and intrinsic functional connectivity, respectively, differ in patients with schizophrenia and major depression, independently from current symptoms. While SN volume loss and DMN aberrant structural connectivity did not differ across groups, patients with schizophrenia had less intrinsic hyperconnectivity between SN and DMN than patients with depression. Results provide first evidence for distinct functional hyperconnectivity between DMN and SN in schizophrenia and depression, potentially reflecting distinct underlying pathophysiological mechanisms.

Multi-modal changes in SN and DMN in schizophrenia and depression

In comparison with healthy controls, both a consistent decrease of regional GMV in the SN and at-trend alterations of inter-regional SC in the DMN was found in patients with schizophrenia and depression, respectively (Table 3,

Table 3 Group comparisons for DMN and SN

Group comparison	Network	iFC		SC		rGMV	
		WBF	P-Value	WBF	P-Value	WBF	P-Value
Patient group vs healthy control group							
HC vs SZP	DMN	-0.294	0.392	0.209	0.005*	1.077	0.146
	SN	3.624	< 0.001**	0.064	0.162	3.753	< 0.001**
	DMN-SN	-2.696	0.0041*	0.032	0.150	–	–
HC vs MDD	DMN	1.323	0.095	0.145	0.037*	0.818	0.207
	SN	3.461	< 0.001**	0.079	0.122	4.030	< 0.001**
	DMN-SN	-5.766	< 0.001**	0.036	0.123	–	–
Patient group vs patient group							
SZP vs MDD	DMN	1.780	0.037*	-0.035	0.351	-0.120	0.450
	SN	-0.353	0.372	0.002	0.473	0.507	0.302
	DMN-SN	-2.937	0.002**	0.002	0.473	–	–

Pairwise group comparisons across groups of healthy controls and patients with major depression and schizophrenia, respectively, by Brunner and Munzel's generalized Wilcoxon rank-sum testing * $p < 0.05$, ** $p < 0.002$ (Bonferroni corrected). Tests among healthy controls and patients were controlled for linear effects of sex, age, and medication via regression analysis, tests among patient groups were additionally controlled for psychiatric symptoms. *iFC* intrinsic functional connectivity, *SC* structural connectivity,*rGMV* regional grey matter volume, W_{BF} Brunner and Munzel's generalized Wilcoxon test statistic, *SZP* schizophrenia, *HC* healthy controls, *MDD* major depressive disorder.

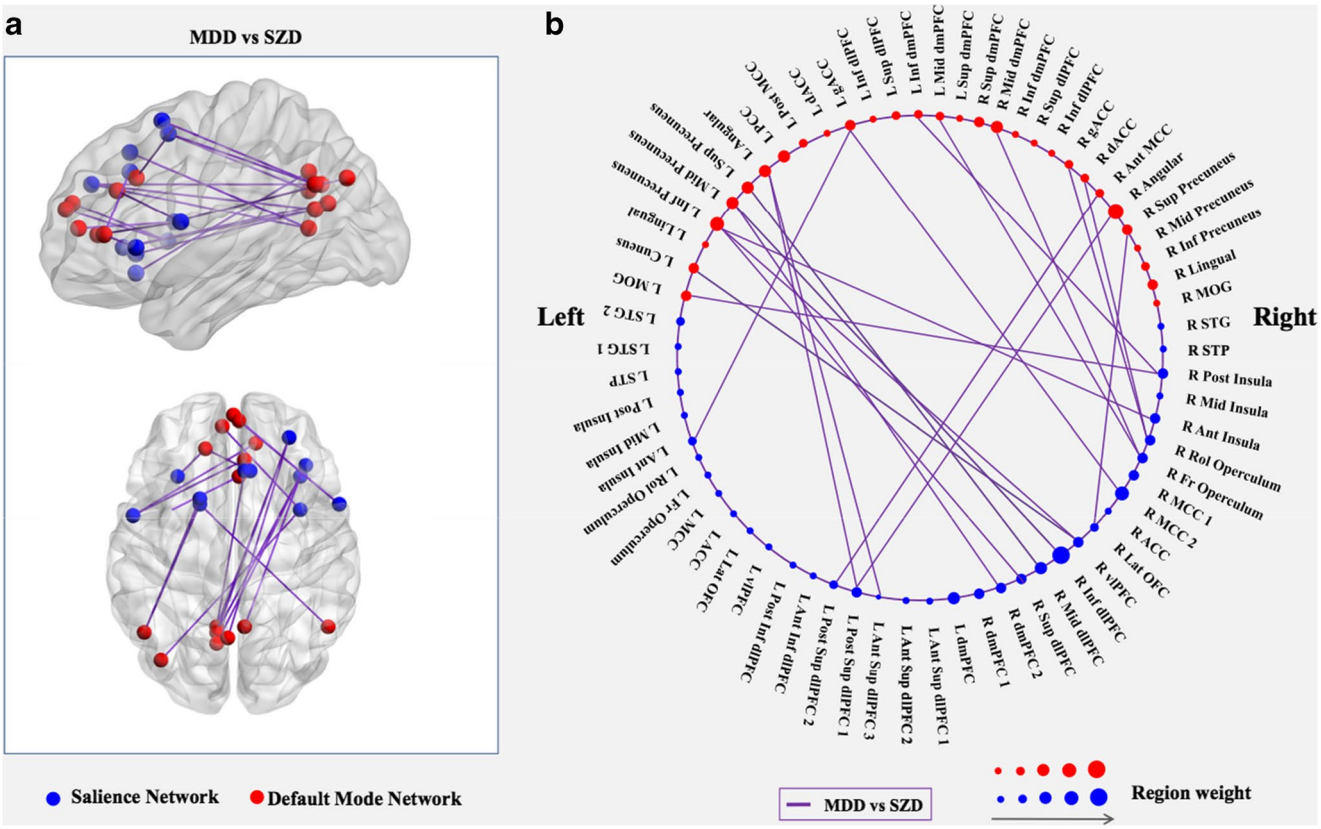

Fig. 3 20 connections with highest discriminative power for change

middle and last columns). These findings are in line with previous studies, which reported robust GMV decrease in SN areas for each disorder (Bora et al. 2012; Ellison-Wright et al. 2008)as well as aberrant SC of white matter tracts related to the DMN, such as cingulum bundle or deep frontal lobe white matter in schizophrenia and major depression (Ellison-Wright et al. 2009). Furthermore, we found both consistently reduced inter-regional iFC within the SN and increased iFC between DMN and SN in each patient group (Table 3, first row). These findings match previous reports about changed intra- and inter-network intrinsic connectivity of these two networks in schizophrenia and major depression, respectively (Orliac et al. 2013; Whitfield-Gabrieli et al. 2009; Wotruba et al. 2014; Kaiser et al. 2015; Manoliu et al. 2013a, b, 2014; Mulders et al. 2015; Greicius et al. 2007; Palaniyappan et al. 2013; Tahmasian et al. 2013). In summary, results indicate consistent multi-modal changes of ongoing interactions and underlying gray and white matter structure of DMN and SN in acute patients with schizophrenia and depression, respectively.

Stronger hyperconnectivity between DMN and SN in depression than schizophrenia

iFC increase between DMN and SN was stronger in patients with depression than in those with schizophrenia (Table 3, first row). Increased hyperconnectivity was independent from current symptoms, which were controlled for. As reduced iFC within the SN did not differ across groups, distinct hyperconnectivity was specific for DMN-SN iFC and not general for iFC changes. The most discriminative SN-DMN iFC connections comprised mainly connections from the fronto-insular SN to the posterior-parietal DMN (Fig. 3).

Previous findings and computational models about iFC demonstrated that emergent spatio-temporal patterns of iFC are based on both regional and inter-regional factors:regional factors concern structure and ongoing activity of local neuronal circuits, inter-regional factors concern the structural connectivity between these local circuits (for example (Deco et al. 2013)). For both regional structure (i.e. GMV of DMN and SN) and inter-regional structural connectivity (i.e. SC between SN and DMN), we did not find differences across patient groups (Table 3), suggesting that in patients with schizophrenia and depression, distinct DMN-SN hyperconnectivity is mainly driven by distinct ongoing activity of local circuits in DMN and SN, respectively.

Neurodynamical models of such local circuit activity show that both regional dynamics of different local pools of excitatory and inhibitory neurons and influences form neuromodulatory transmitters critically shape emergent iFC (Deco et al. 2013). Consequently, these models suggest that distinct changes in the balance between excitatory and inhibitory activity and/or in neuromodulatory activity might underlie distinct DMN-SN hyperconnectivity in schizophrenia and depression. Concerning the balance between excitatory and inhibitory activity, previous studies demonstrated dependence of DMN iFC on glutamate and GABA levels, respectively (Duncan et al. 2014). Critically, studies in patients demonstrate that these relations are altered in both major depression (Walter et al. 2009) and schizophrenia (Kraguljac et al. 2013). Therefore, distinctively altered balance between glutamate- and GABA-ergic activities might be a candidate for distinct intrinsic hyperconnectivity in schizophrenia and depression (Northoff et al. 2014). Furthermore, concerning neuromodulatory activity, previous studies have shown that, for example, striatal dopamine levels modulate cortical iFC of SN and DMN (Cole et al. 2013). Striatal dopamine levels are increased in schizophrenia (Howes et al. 2011) and decreased in major depression (Bragulat et al. 2007). Therefore, distinct effects of altered dopamine may impact distinctively altered DMN-SN iFC in depression and schizophrenia. Based on these examples, our result of distinct DMN-SN hyperconnectivity in schizophrenia and depression suggests future multi-modal studies in schizophrenia and depression to test these specific hypotheses about underlying factors of distinctively altered DMN-SN iFC.

SN gray matter volume reductions did not differ among patients

In contrast to DMN-SN intrinsic hyperconnectivity, patients' structural changes (i.e. GMV decrease in SN and aberrant SC in the DMN) as well as reduced iFC within the SN did not differ between disorders (Table 3, last row). These findings are independent of confounding factors like current medication or symptoms, which we controlled for. Concerning GMV, our result is in line with a recent finding of consistently reduced GMV specifically in the SN across several psychiatric disorders including major depression and schizophrenia (Goodkind et al. 2015). Accounting for the focus of changes on the SN, these findings suggest that changes in the SN, including volume loss and reduced iFC, might be rather robust features of schizophrenia and depression.

Conclusion

The current study provides evidence for distinct functional hyperconnectivity between DMN and SN in schizophrenia and major depression, while structural changes in DMN and SN were similar. Distinct hyperconnectivity may reflect different pathophysiological mechanisms for DMN-SN interactions in schizophrenia and depression.

Author Contributions JS and CS designed the study; CM, MT, AM, MS and DS recruited participants and acquired data; JB and HF

acquired data; JS, QY, GL, CL, DY and LG analysed data; CZ, VR, AW and CS interpreted data; JS and CS drafted the article; all authors critically revised and approved the final version of the article.

Funding This study was supported by the National Natural Science Foundation of China (61403062, 61433014 to J.S.), China Postdoctoral Science Foundation (2015M580786 to J.S., 2014M552344, 2015T80973 to Q.Y.), Science-Technology Foundation for Young Scientist of SiChuan Province (2016JQ0007 to J.S.) and the German Federal Ministry of Education and Research (BMBF 01EV0710 to A.M.W., BMBF 01ER0803 to C.S.)

Compliance with Ethical Standards

Conflict of interest The authors declare no conflict of interest.

Ethical approval All procedures performed in studies involving human participants were in accordance with the ethical standards of the institutional and/or national research committee and with the 1964 Helsinki declaration and its later amendments or comparable ethical standards.

Informed consent Informed consent was obtained from all individual participants included in the study.

References

Abou-Elseoud, A., Starck, T., Remes, J., Nikkinen, J., Tervonen, O., & Kiviniemi, V. (2010). The effect of model order selection in group PICA. *Human Brain Mapping, 31*(8), 1207–1216.

Allen, E. A., Erhardt, E. B., Damaraju, E., Gruner, W., Segall, J. M., Silva, R. F., et al. (2011). A baseline for the multivariate comparison of resting-state networks. *Frontiers in Systems Neuroscience, 5*, 2.

American Psychiatric Association. (2000). DSM-IV-TR: Diagnostic and statistical manual of mental disorders, text revision. Washington, DC: American Psychiatric Association, 75.

Biswal, B., Zerrin Yetkin, F., Haughton, V. M., & Hyde, J. S. (1995). Functional connectivity in the motor cortex of resting human brain using echo-planar mri. *Magnetic Resonance in Medicine, 34*(4), 537–541.

Bora, E., Fornito, A., Pantelis, C., & Yücel, M. (2012). Gray matter abnormalities in major depressive disorder: a meta-analysis of voxel based morphometry studies. *Journal of Affective Disorders, 138*(1), 9–18.

Borgwardt, S. J., McGUIRE, P. K., Aston, J., Berger, G., Dazzan, P., Gschwandtner, U. T. E., et al. (2007). Structural brain abnormalities in individuals with an at-risk mental state who later develop psychosis. *The British Journal of Psychiatry, 191*(51), s69-s75.

Bragulat, V., Paillère-Martinot, M. L., Artiges, E., Frouin, V., Poline, J. B., & Martinot, J. L. (2007). Dopaminergic function in depressed patients with affective flattening or with impulsivity:[18 F] fluoro-L-dopa positron emission tomography study with voxel-based analysis. *Psychiatry Research: Neuroimaging, 154*(2), 115–124.

Brunner, E., & Munzel, U. (2000). The nonparametric Behrens-Fisher problem: asymptotic theory and a small-sample approximation. *Biometrical Journal, 42*(1), 17–25.

Buchsbaum, M. S., Schoenknecht, P., Torosjan, Y., Newmark, R., Chu, K. W., Mitelman, S., et al. (2006). Diffusion tensor imaging of frontal lobe white matter tracts in schizophrenia. *Annals of General Psychiatry, 5*(1), 19.

Chen, X., Duan, M., Xie, Q., Lai, Y., Dong, L., Cao, W., et al. (2015). Functional disconnection between the visual cortex and the sensorimotor cortex suggests a potential mechanism for self-disorder in schizophrenia. *Schizophrenia Research, 166*(1), 151–157.

Cole, D. M., Oei, N. Y., Soeter, R. P., Both, S., van Gerven, J. M., Rombouts, S. A., & Beckmann, C. F. (2013). Dopamine-dependent architecture of cortico-subcortical network connectivity. *Cerebral Cortex, 23*(7), 1509–1516.

Corbetta, M., & Shulman, G. L. (2002). Control of goal-directed and stimulus-driven attention in the brain. *Nature Reviews Neuroscience, 3*(3), 201–215.

Deco, G., Jirsa, V. K., & McIntosh, A. R. (2013). Resting brains never rest: computational insights into potential cognitive architectures. *Trends in Neurosciences, 36*(5), 268–274.

Dong, D., Wang, Y., Chang, X., Luo, C., & Yao, D. (2017). Dysfunction of large-scale brain networks in Schizophrenia: a meta-analysis of resting-state functional connectivity. Schizophrenia bulletin, sbx034.

Duncan, N. W., Wiebking, C., & Northoff, G. (2014). Associations of regional GABA and glutamate with intrinsic and extrinsic neural activity in humans—A review of multimodal imaging studies. *Neuroscience & Biobehavioral Reviews, 47*, 36–52.

Ellison-Wright, I., & Bullmore, E. (2009). Meta-analysis of diffusion tensor imaging studies in schizophrenia. *Schizophrenia Research, 108*(1), 3–10.

Ellison-Wright, I., Glahn, D. C., Laird, A. R., Thelen, S. M., & Bullmore, E. (2008). The anatomy of first-episode and chronic schizophrenia: an anatomical likelihood estimation meta-analysis. *American Journal of Psychiatry, 165*(8), 1015–1023.

Fox, M. D., & Raichle, M. E. (2007). Spontaneous fluctuations in brain activity observed with functional magnetic resonance imaging. *Nature Reviews Neuroscience, 8*(9), 700–711.

Frodl, T. S., Koutsouleris, N., Bottlender, R., Born, C., Jäger, M., Scupin, I., … Meisenzahl, E. M. (2008). Depression-related variation in brain morphology over 3 years: effects of stress? *Archives of General Psychiatry, 65*(10), 1156–1165.

Goodkind, M., Eickhoff, S. B., Oathes, D. J., Jiang, Y., Chang, A., Jones-Hagata, L. B., et al. (2015). Identification of a common neurobiological substrate for mental illness. *JAMA Psychiatry, 72*(4), 305–315.

Greicius, M. D., Flores, B. H., Menon, V., Glover, G. H., Solvason, H. B., Kenna, H., et al. (2007). Resting-state functional connectivity in major depression: abnormally increased contributions from subgenual cingulate cortex and thalamus. *Biological Psychiatry, 62*(5), 429–437.

Greicius, M. D., Krasnow, B., Reiss, A. L., & Menon, V. (2003). Functional connectivity in the resting brain: a network analysis of the default mode hypothesis. *Proceedings of the National Academy of Sciences*, 100(1), 253–258.

Hagmann, P., Cammoun, L., Gigandet, X., Meuli, R., Honey, C. J., Wedeen, V. J., & Sporns, O. (2008). Mapping the structural core of human cerebral cortex. PLoS Biolology, 6(7), e159.

Hahn, K., Myers, N., Prigarin, S., Rodenacker, K., Kurz, A., Förstl, H., et al. (2013). Selectively and progressively disrupted structural connectivity of functional brain networks in Alzheimer's disease—revealed by a novel framework to analyze edge distributions of networks detecting disruptions with strong statistical evidence. *Neuroimage, 81*, 96–109.

Hamilton, J. P., Chen, M. C., & Gotlib, I. H. (2013). Neural systems approaches to understanding major depressive disorder: an intrinsic functional organization perspective. *Neurobiology of Disease, 52*, 4–11.

Hamilton, M. (1960). A rating scale for depression. *Journal of Neurology, Neurosurgery & Psychiatry, 23*(1), 56–62.

Howes, O. D., Bose, S. K., Turkheimer, F., Valli, I., Egerton, A., Valmaggia, L. R., et al. (2011). Dopamine synthesis capacity before onset of psychosis: a prospective [18F]-DOPA PET imaging study. *American Journal of Psychiatry, 168*(12), 1311–1317.

Kaiser, R. H., Andrews-Hanna, J. R., Wager, T. D., & Pizzagalli, D. A. (2015). Large-scale network dysfunction in major depressive disorder: a meta-analysis of resting-state functional connectivity. *JAMA Psychiatry, 72*(6), 603–611.

Kay, S. R., Flszbein, A., & Opfer, L. A. (1987). The positive and negative syndrome scale (PANSS) for schizophrenia. *Schizophrenia Bulletin, 13*(2), 261.

Kieseppä, T., Eerola, M., Mäntylä, R., Neuvonen, T., Poutanen, V. P., Luoma, K., et al. (2010). Major depressive disorder and white matter abnormalities: a diffusion tensor imaging study with tract-based spatial statistics. *Journal of Affective Disorders, 120*(1), 240–244.

Kraguljac, N. V., White, D. M., Reid, M. A., & Lahti, A. C. (2013). Increased hippocampal glutamate and volumetric deficits in unmedicated patients with schizophrenia. *JAMA Psychiatry, 70*(12), 1294–1302.

Lazar, M., Weinstein, D. M., Tsuruda, J. S., Hasan, K. M., Arfanakis, K., Meyerand, M. E., et al. (2003). White matter tractography using diffusion tensor deflection. *Human Brain Mapping, 18*(4), 306–321.

Liao, Y., Huang, X., Wu, Q., Yang, C., Kuang, W., Du, M., et al. (2013). Is depression a disconnection syndrome? Meta-analysis of diffusion tensor imaging studies in patients with MDD. *Journal of Psychiatry & Neuroscience: JPN, 38*(1), 49.

Luo, C., Zhang, Y., Cao, W., Huang, Y., Yang, F., Wang, J., et al. (2015). Altered structural and functional feature of striato-cortical circuit in benign epilepsy with centrotemporal spikes. *International Journal of Neural Systems, 25*(06), 1550027.

Manoliu, A., Meng, C., Brandl, F., Doll, A., Tahmasian, M., Scherr, M., et al. (2013a). Insular dysfunction within the salience network is associated with severity of symptoms and aberrant inter-network connectivity in major depressive disorder. *Frontiers in Human Neuroscience, 7*, 930. https://doi.org/10.3389/fnhum.2013.00930.

Manoliu, A., Riedl, V., Doll, A., Bäuml, J. G., Mühlau, M., Schwerthöffer, D., et al. (2013b). Insular dysfunction reflects altered between-network connectivity and severity of negative symptoms in schizophrenia during psychotic remission. *Frontiers in Human Neuroscience, 7*, 216.

Manoliu, A., Riedl, V., Zherdin, A., Mühlau, M., Schwerthöffer, D., Scherr, M., et al. (2014). Aberrant dependence of default mode/central executive network interactions on anterior insular salience network activity in schizophrenia. *Schizophrenia Bulletin, 40*(2), 428–437.

Meng, C., Brandl, F., Tahmasian, M., Shao, J., Manoliu, A., Scherr, M., et al. (2013). Aberrant topology of striatum's connectivity is associated with the number of episodes in depression. *Brain, 137*, 598–609.

Menon, V. (2011). Large-scale brain networks and psychopathology: a unifying triple network model. *Trends in Cognitive Sciences, 15*(10), 483–506.

Mulders, P. C., van Eijndhoven, P. F., Schene, A. H., Beckmann, C. F., & Tendolkar, I. (2015). Resting-state functional connectivity in major depressive disorder: a review. *Neuroscience & Biobehavioral Reviews, 56*, 330–344.

Northoff, G., & Sibille, E. (2014). Cortical GABA neurons and self-focus in depression: a model linking cellular, biochemical, and neural network findings. *Molecular Psychiatry, 19*(9), 959.

Orliac, F., Naveau, M., Joliot, M., Delcroix, N., Razafimandimby, A., Brazo, P., et al. (2013). Links among resting-state default-mode network, salience network, and symptomatology in schizophrenia. *Schizophrenia Research, 148*(1), 74–80.

Palaniyappan, L., & Liddle, P. F. (2012). Does the salience network play a cardinal role in psychosis? An emerging hypothesis of insular dysfunction. *Journal of Psychiatry & Neuroscience: JPN, 37*, 17–27.

Palaniyappan, L., Simmonite, M., White, T. P., Liddle, E. B., & Liddle, P. F. (2013). Neural primacy of the salience processing system in schizophrenia. *Neuron, 79*(4), 814–828.

Pessoa, L. (2014). Brain networks: Moving beyond graphs. Reply to comments on ``understanding brain networks and brain organization''. *Physics of Life Reviews, 11*, 462–466.

Schmidt, A., Diwadkar, V. A., Smieskova, R., Harrisberger, F., Lang, U. E., McGuire, P., et al. (2014). Approaching a network connectivity-driven classification of the psychosis continuum: a selective review and suggestions for future research. *Frontiers in Human Neuroscience, 8*, 1047.

Seeley, W. W., Menon, V., Schatzberg, A. F., Keller, J., Glover, G. H., Kenna, H., et al. (2007). Dissociable intrinsic connectivity networks for salience processing and executive control. *Journal of Neuroscience, 27*(9), 2349–2356.

Shao, J., Myers, N., Yang, Q., Feng, J., Plant, C., Böhm, C., et al. (2012). Prediction of Alzheimer's disease using individual structural connectivity networks. *Neurobiology of Aging, 33*(12), 2756–2765.

Sheline, Y. I., Price, J. L., Yan, Z., & Mintun, M. A. (2010). Resting-state functional MRI in depression unmasks increased connectivity between networks via the dorsal nexus. *Proceedings of the National Academy of Sciences*, 107(24), 11020–11025.

Sorg, C., Manoliu, A., Neufang, S., Myers, N., Peters, H., Schwerthöffer, D., et al. (2013). Increased intrinsic brain activity in the striatum reflects symptom dimensions in schizophrenia. *Schizophrenia Bulletin, 39*(2), 387–395.

Spitzer, R. L., Williams, J. B., Gibbon, M., & First, M. B. (1992). The structured clinical interview for DSM-III-R (SCID): I: history, rationale, and description. *Archives of General Psychiatry, 49*(8), 624–629.

Stephan, K. E., Friston, K. J., & Frith, C. D. (2009). Dysconnection in schizophrenia: from abnormal synaptic plasticity to failures of self-monitoring. *SchizophreniaBulletin, 35*, 509–527.

Tahmasian, M., Knight, D. C., Manoliu, A., Schwerthöffer, D., Scherr, M., Meng, C., et al. (2013). Aberrant intrinsic connectivity of hippocampus and amygdala overlap in the fronto-insular and dorsomedial-prefrontal cortex in major depressive disorder. *Frontiers in Human Neuroscience, 7*, 639.

Uddin, L. Q., Supekar, K. S., Ryali, S., & Menon, V. (2011). Dynamic reconfiguration of structural and functional connectivity across core neurocognitive brain networks with development. *Journal of Neuroscience, 31*(50), 18578–18589.

van den Heuvel, M. P., & Fornito, A. (2014). Brain networks in schizophrenia. *Neuropsychology Review, 24*(1), 32–48.

Van Dijk, K. R., Sabuncu, M. R., & Buckner, R. L. (2012). The influence of head motion on intrinsic functional connectivity MRI. *Neuroimage, 59*(1), 431–438.

Walter, M., Henning, A., Grimm, S., Schulte, R. F., Beck, J., Dydak, U., et al. (2009). The relationship between aberrant neuronal activation in the pregenual anterior cingulate, altered glutamatergic metabolism, and anhedonia in major depression. *Archives of General Psychiatry, 66*(5), 478–486.

Wang, D., Zhou, Y., Zhuo, C., Qin, W., Zhu, J., Liu, H., et al. (2015). Altered functional connectivity of the cingulate subregions in schizophrenia. *Translational Psychiatry*, 5(6), e575.

Whitfield-Gabrieli, S., Thermenos, H. W., Milanovic, S., Tsuang, M. T., Faraone, S. V., McCarley, R. W., et al. (2009). Hyperactivity and hyperconnectivity of the default network in schizophrenia and in first-degree relatives of persons with schizophrenia. *Proceedings of the National Academy of Sciences*, 106(4), 1279–1284.

Williamson, P. (2007). Are anticorrelated networks in the brain relevant to schizophrenia? *Schizophrenia Bulletin, 33*(4), 994–1003.

Wotruba, D., Michels, L., Buechler, R., Metzler, S., Theodoridou, A., Gerstenberg, M., et al. (2013). Aberrant coupling within and across the default mode, task-positive, and salience network in subjects at risk for psychosis. *Schizophrenia Bulletin, 40*, 1095–1104.